

# UC Davis

## UC Davis Previously Published Works

### Title

Reduction in Wound Bioburden using a Silver-Loaded Dissolvable Microfilm Construct

### Permalink

<https://escholarship.org/uc/item/3939g1mm>

### Journal

Advanced Healthcare Materials, 3(6)

### ISSN

2192-2640

### Authors

Herron, Maggie  
Agarwal, Ankit  
Kierski, Patricia R  
et al.

### Publication Date

2014-06-01

### DOI

10.1002/adhm.201300537

Peer reviewed



Published in final edited form as:

*Adv Healthc Mater.* 2014 June ; 3(6): 916–928. doi:10.1002/adhm.201300537.

## Reduction in Wound Bioburden using a Silver-Loaded Dissolvable Microfilm Construct

**Maggie Herron<sup>#</sup>,**

Department of Chemical and Biological Engineering, University of Wisconsin, 1415 Engineering Drive, Madison, WI 53706 (USA)

**Dr. Ankit Agarwal<sup>#</sup>,**

Department of Chemical and Biological Engineering, University of Wisconsin, 1415 Engineering Drive, Madison, WI 53706 (USA)

**Patricia R. Kierski,**

Department of Surgery, School of Veterinary Medicine, University of Wisconsin-Madison, 2015 Linden Dr., Madison, WI 53706 (USA)

**Diego F. Calderon,**

Department of Surgery, School of Veterinary Medicine, University of Wisconsin-Madison, 2015 Linden Dr., Madison, WI 53706 (USA)

**Dr. Leandro B. C. Teixeira,**

Department of Pathobiology, School of Veterinary Medicine, University of Wisconsin-Madison, 2015 Linden Dr, Madison, WI 53706 (USA)

**Prof. Michael J. Schurr,**

Department of Surgery, School of Medicine, University of Colorado-Denver, 12631 E. 17<sup>th</sup> Avenue, Aurora, CO 80045 (USA)

**Prof. Christopher J. Murphy,**

Department of Ophthalmology and Vision Sciences, School of Medicine, Department of Surgical and Radiological Sciences, School of Veterinary Medicine, University of California-Davis, 1423 Tupper Hall, Davis, CA 95616 (USA)

**Prof. Charles J. Czuprynski,**

Department of Pathobiology, School of Veterinary Medicine, University of Wisconsin-Madison, 2015 Linden Dr, Madison, WI 53706 (USA)

**Prof. Jonathan F. McAnulty, and**

Department of Surgery, School of Veterinary Medicine, University of Wisconsin-Madison, 2015 Linden Dr., Madison, WI 53706 (USA)

**Prof. Nicholas L. Abbott**

---

Correspondence to: Charles J. Czuprynski, [czuprync@svm.vetmed.wisc.edu](mailto:czuprync@svm.vetmed.wisc.edu); Jonathan F. McAnulty, [mcanultj@svm.vetmed.wisc.edu](mailto:mcanultj@svm.vetmed.wisc.edu); Nicholas L. Abbott, [abbott@enr.wisc.edu](mailto:abbott@enr.wisc.edu).

<sup>#</sup>Authors contributed equally

Supporting Information

Supporting Information is available online from the Wiley Online Library or from the author.

Department of Chemical and Biological Engineering, University of Wisconsin, 1415 Engineering Drive, Madison, WI 53706 (USA)

Charles J. Czuprynski: czuprync@svm.vetmed.wisc.edu; Jonathan F. McNulty: mcanultj@svm.vetmed.wisc.edu; Nicholas L. Abbott: abbot@enr.wisc.edu

## Abstract

Silver is a widely used antimicrobial agent, yet when impregnated in macroscopic dressings, it stains wounds, can lead to tissue toxicity and can inhibit healing. Recently, we reported that polymeric nanofilms containing silver nanoparticles exhibit antimicrobial activity at loadings and release rates of silver that are 100x lower than conventional dressings. Here we report fabrication of composite microfilm constructs that provide a facile way to transfer the silver-loaded polymeric nanofilms onto wounds *in vivo*. The construct is fabricated from a silver nanoparticle-loaded polymeric nanofilm that is laminated with a micrometer-thick soluble film of polyvinylalcohol (PVA). When placed on a moist wound, the PVA dissolves, leaving the silver-loaded nanofilm immobilized on the wound-bed. *In vitro*, the immobilized nanofilms release  $<1 \mu\text{g cm}^{-2}/\text{day}$  of silver over 30 days from skin-dermis and they kill  $5 \log_{10}$  CFUs of *Staphylococcus aureus* in 24 h. In mice, wounds inoculated with  $10^5$  CFU *S. aureus* presented up to  $3 \log_{10}$  less bacterial burden when treated with silver/nanofilms for 3 days, as compared to unmodified wounds. In uncontaminated wounds, silver/nanofilms allow normal and complete wound closure by re-epithelialization. We conclude that dissolvable microfilm constructs may overcome key limitations associated with current uses of silver in wound healing.

## Keywords

Microfilms; silver; polymers; wound healing; bacteria

## 1. Introduction

Microbial colonization of wounds can result in delayed wound healing<sup>[1]</sup> in both acute wounds such as surgical incisions and burns<sup>[2]</sup> and chronic wounds<sup>[3]</sup> such as diabetic and venous ulcers. Recent advances aimed at improvement of management of microbial colonization of wounds include the use of advanced polymeric dressings,<sup>[4]</sup> scaffolds, and hydrogels<sup>[5]</sup> that provide long-term release of broad spectrum antimicrobial agents such as silver,<sup>[6]</sup> chlorhexidine,<sup>[7]</sup> polyhexamethylene biguanide (PHMB),<sup>[8]</sup> and povidone iodine.<sup>[9]</sup> However, these formulations rely on diffusion of active agents from a macroscopic reservoir within the dressing and result in accumulation of large quantities of antimicrobial agents in the wound tissue, which has been documented in some studies to cause either tissue staining,<sup>[10]</sup> tissue toxicity<sup>[11,12]</sup> and/or impaired wound healing.<sup>[13]</sup> In particular, Burd et al. documented significant inhibition of re-epithelialization in full-thickness murine wounds treated with four commercially available silver dressings.<sup>[14]</sup> Clinical guidelines, therefore, recommend the use of silver dressings “for wounds where infection is already established, or an excessive wound bioburden is delaying healing (‘critical colonization’), and that they be used for short periods (less than 2 weeks) before re-evaluation.”<sup>[15]</sup>

Motivated by the challenges of managing microbial burden of wounds, we recently described a new approach for the delivery of antibacterial and bioactive agents to wound-beds. [16,17] The approach involves modification of wound-beds with polymeric nanofilms that provide localized release of bioactive agents in the wound microenvironment. When using antimicrobials, agent release from the nanofilms at the site of potential bacterial colonization leads to antimicrobial efficacy at 100x lower release rates as compared to conventional dressings for which antimicrobials have to diffuse through wound-fluids to reach the site of action at the wound bed. In this study, as a prototypical but important example, we demonstrate efficacy of polymer nanofilms containing silver nanoparticles for management of microbial colonization of wounds. The principles are, however, generalizable and applicable to other antimicrobial and bioactive agents.

The nanofilms used in our study were fabricated as interpenetrated polyelectrolyte multilayers (PEMs) by the layer-by layer (LbL) assembly of two oppositely charged polyelectrolytes; poly(allylamine hydrochloride), (PAH), and poly(acrylic acid), (PAA). LbL assembly is simple and applicable to many different polyelectrolytes (either synthetic<sup>[18,19]</sup> or natural<sup>[20,21]</sup>) and has been investigated for the surface modification of several biomedical devices.<sup>[22]</sup> Post-fabrication, we impregnated the PEMs used in our study with a range of loadings of silver nanoparticles by silver-ion exchange and *in situ* reduction, as reported elsewhere.<sup>[23,24]</sup> Because the fabrication and impregnation of PEMs directly on wound-beds is impractical due to the laborious and time-consuming fabrication procedure (and nature of some reagents), we recently demonstrated that silver-nanoparticle impregnated PEMs prefabricated on elastomeric sheets of polydimethylsiloxane (PDMS) could be stamped mechanically on soft-tissues such as human skin dermis.<sup>[16]</sup> In that approach, microspheres incorporated into the PEMs facilitated the transfer of PEMs onto the soft tissues. We documented that immobilization of silver/PEMs onto dermis (of human cadaver skin grafts) provided sustained release of silver-ions that killed more than 5 log<sub>10</sub> CFUs of bacteria in solutions incubated with the dermis. Although this approach was effective for transfer of PEMs on to flat surfaces, we also found that it was sometimes impractical to mechanically stamp PEMs onto excisional wounds in small animals due to variances in wound surface topography, stiffness and lubricity of the tissues. Specifically, because of variance in the rigidity of tissue/organs under the wound-tissue, the stamping procedure would sometimes result in non-uniform transfer of the nanofilms onto wound tissue. To overcome that problem, we present herein the outcome of an investigation of the use a sacrificial, water-soluble, polymeric support layer<sup>[25–27]</sup> for the facile transfer of silver-loaded polymer nanofilms onto wound tissue. We spin-coated the non-toxic polymer polyvinylalcohol (PVA) over PEMs fabricated on PDMS, and demonstrate that the PEM/PVA construct can be peeled from the PDMS to form an easily handled composite “microfilm”.<sup>[26]</sup> The PVA layer of the PEM/PVA microfilm dissolves quickly on a moist surface leaving the PEM nanofilm immobilized on the surface, as illustrated in Figure 1. We use this approach for the modification of murine wound-beds, test the persistence of PEMs on the wound-beds and the release rates of silver from the nanofilms, and evaluate the ability of silver-loaded PEMs to both reduce microbial colonization in contaminated wounds under primary dressings and promote normal wound healing. The current study is focused

on delivery of silver to wound beds because silver is an important and widely adopted antimicrobial agent and it does not lead to antibiotic resistance.

## 2. Results

### 2.1. Fabrication of free standing PEM/PVA microfilms

Layer-by-layer deposition was used to fabricate PEMs consisting of PAH (pH 7.5) and PAA (pH 2.5 and 5.5), starting with deposition of a layer of PAH on a poly(dimethylsiloxane) (PDMS) sheet (see Experimental section for details). Below, we denote the PEMs as  $(\text{Poly1}_{\text{pH1}}/\text{Poly2}_{\text{pH2}})_n$ , where Poly1 and Poly2 are the polymers used and pH1 and pH2 are the respective solution conditions at which those polymers were adsorbed;  $n$  is the number of bilayers, where one bilayer consists of one adsorbed layer of Poly1 and one adsorbed layer of Poly2. Here, we also note that it is understood that the layers of such “bilayers” are substantially intermixed in PEMs. We confirmed growth of  $(\text{PAH}_{7.5}/\text{PAA}_{2.5 \text{ and } 5.5})_{10.5}$  multilayers (vacuum dried after fabrication) on piranha-cleaned silicon wafers by performing measurements of ellipsometric thicknesses (Figure S1).

PVA is a non-toxic biodegradable polymer widely used in fabrication of biomaterials including hydrogels.<sup>[28,29]</sup> PVA with MW = 22 kDa was employed in our studies so that any polymer absorbed systemically would be removed through renal filtration.<sup>[30]</sup> To assemble the microfilms, 25–50  $\mu\text{L}$  of 2.5 wt.% PVA solution was pipetted over PEMs supported on PDMS sheets (6–8 mm diameter), wetting all their surface area. The PDMS disk was subsequently spun at 1500 rpm ( $ac = 27$ ) for 10 s to facilitate deposition of a uniformly thick microfilm of PVA over the PEM. Next, the microfilm construct was dried in an oven for 5 min at 70°C. After drying, the composite PEM/PVA construct was peeled from the PDMS surface using tweezers. The thickness of the PVA microfilm was measured to be 20–40  $\mu\text{m}$ , using an electric digital micrometer (Marathon Watch Co., Richmond Hill, Ont., Canada). The final PEM/PVA microfilm was measured to have an elastic Young’s modulus ( $E'$ ) of 1 GPa (Figure S2). The microfilms were sufficiently robust that they could be easily handled by hand or tweezers and placed on wound surfaces or skin grafts.

The effectiveness of the removal of PEMs from the PDMS sheets was quantified using  $(\text{PAH}/\text{PAA}_{5.5})_{10.5}$  nanofilms that were assembled with fluorescein-5-isothiocyanate (FITC) (Ext/Em-492/518)-labeled PAH. Figure 2a–c show montage fluorescent micrographs of a PEM/PVA microfilm before and after peeling from the PDMS substrate. The fluorescent micrographs (imaged using 4x objective) were stitched together using MosaicJ, a plugin available in Fiji software, to create a composite image of the polymer film over a large area (6 mm diameter). The results demonstrate that  $99.3 \pm 1.1$  % of the PEM was peeled from the PDMS sheet (quantified using fluorescent area from micrographs using Fiji software, averaged over 23 samples). Here we make several additional comments regarding this process. First, we emphasize that the results reported above were highly reproducible, and were obtained using multiple batches of PEMs and PVA. Second, we observed that PEMs fabricated on bare glass and coated with PVA could not be peeled from the glass substrates. However, if the glass substrates were functionalized with octadecyltrichlorosilane (OTS) before deposition of the PEMs, it was possible to peel the PEM/PVA microfilm from the

rigid substrate (see Figure S3). This result is consistent with OTS treatment of the glass leading to a low energy surface that only weakly adheres to the PEMs.<sup>[25,26]</sup>

After fabrication, PEMs were impregnated with silver by the exchange of silver ions with protons of the carboxylic groups of the PAA in the PEMs. The silver ions in the PEMs were subsequently reduced *in situ* to form silver nanoparticles (see Experimental Section for details). The silver loading in each PEM was tailored by controlling: (i) the number of bilayers in the PEM, (ii) pH of the assembly solution of the weak polyelectrolyte PAA (pH = 5.5 or pH = 2.5), and (iii) the number of silver ion exchange and reduction cycles. For *in vitro* studies, PEMs with a single cycle of silver ion exchange and reduction were tested and characterized for short-term (1 – 4 days) silver release profiles and antibacterial efficacy. Constructs identified from the *in vitro* studies were impregnated with higher silver loadings by using multiple silver ion exchange and reduction cycles to provide long-term (>10 days) release of antibacterial silver in murine wounds. In this study, silver ions within PEMs were reduced to silver nanoparticles through multiple cycles of silver ion exchange and reduction to increase the total silver loading within the PEMs and to provide sustained release of antimicrobial but non-cytotoxic levels of silver ions. As shown in Figure 2d, consistent with prior studies,<sup>[17]</sup> the loading of silver in PEMs of (PAH/PAA)<sub>10.5</sub> could be varied systematically from  $0.04 \pm <0.01$  to  $2.9 \pm 0.1 \mu\text{g cm}^{-2}$  by changing the pH of the PAA assembly solution from pH 5.5 to pH 2.5. The PEMs comprised of (PAH/PAA<sub>2.5</sub>)<sub>5.5</sub> provided intermediate loadings of silver ( $1.3 \pm 0.01 \mu\text{g cm}^{-2}$ ). We chose these PEMs with 3 different loadings of silver for further *in vitro* antibacterial testing. We note that the  $0.04 \pm <0.01 \mu\text{g cm}^{-2}$  loading was chosen as a control as the PEMs were subjected to the same processing conditions as the other two loadings yet contain minimal active agent. Figure S4 shows that the loadings of silver within the PEMs were measured to be invariant during three months of storage.

We also quantified the amount of silver that remained on the PDMS sheets after peeling of the PEM/PVA composite microfilms from the PDMS (second column of Figure 2d). For all silver loadings used in this study, only trace amounts of silver were determined to remain on the PDMS ( $<0.01$ ,  $0.05 \pm <0.01$  and  $0.07 \pm <0.01 \mu\text{g cm}^{-2}$ , respectively, for the three loadings described above). The loadings of silver in the free standing PEM/PVA composite microfilms were determined to be  $0.04 \pm <0.01$ ,  $1.2 \pm 0.04$ , and  $2.7 \pm 0.2 \mu\text{g cm}^{-2}$ , respectively (third column of Figure 2d). These results suggest that most ( $93 \pm 3 \%$ ,  $95 \pm 4 \%$ , and  $94 \pm 8 \%$ , respectively) of the silver present within the PEMs on the PDMS support was retained in the free-standing PEM/PVA microfilms.

## 2.2. Transfer of PEMs onto Skin Grafts

To simulate the mechanical characteristics and surface topography of a partial thickness wound, we tested the transfer of PEMs onto the dermal side of terminally irradiated human cadaver skin grafts (GammaGraft®, Promethean Lifesciences). To this end, PEM/PVA microfilms with diameter of 6mm were peeled from PDMS sheets and were placed onto the moist skin dermis (6 or 8 mm diameter), with the PEMs facing the surface of the tissue. The skin dermis was maintained moist before the placement of the free standing PEM/PVA microfilm using PBS, mimicking moist wounds. PEM/PVA microfilms that were held by

tweezers (with PEMs side facing the skin dermis) were contacted with the dermis by first placing an edge of the microfilm into contact with the skin dermis and then releasing the microfilm from the tweezers to allow the rest of the microfilm to adhere to the skin dermis. The PVA cast of each microfilm was observed to dissolve gradually over 10 minutes on the moist dermis and the PEMs were observed to adhere to the dermis.

The efficiency of transfer of the PEMs from the PDMS support onto the skin dermis was evaluated using fluorescent microscopy. To enable visualization of fluorescent PEMs over the background auto-fluorescence of the skin graft, PEMs with 40.5 multilayers of FITC-PAH were assembled. Fluorescent imaging was performed immediately after the PEMs were transferred onto the skin dermis. Quantification of the transfer efficiency was performed using Fiji software by comparing the projected fluorescent area of the PEMs on the PDMS sheets (shown in Figure 3a) with that of the PEMs after transfer onto the skin dermis (shown in Figure 3b), averaged over 13 samples. Repeat experiments confirmed that  $99.7 \pm 0.5\%$  of the fluorescent area that was projected by the PEMs on the PDMS sheets was transferred onto the skin dermis. The experiments were performed on several different days using different batches of microfilms.

The rate of dissolution of the PVA cast within a composite microfilm was studied in excess PBS using a Malachite Green spectroscopic dye (0.01 wt% dye) mixed into the PVA solution used for casting. The 8 mm diameter composite microfilms were incubated in a multiwell plate in 3 mL PBS, and the cumulative concentration of Malachite Green that was released into the PBS was determined at different time points by measuring the absorbance of the solution at 595 nm wavelength, as shown in Figure S5. From these measurements, we concluded that  $\sim 98\%$  of the PVA cast dissolves within 10 min of contact with the PBS.

The persistence of the PEMs that were immobilized on the skin-dermis following dissolution of PVA was evaluated using fluorescent microscopy. The fluorescent PEMs were observed to remain adhered to the skin-dermis after repeated pipetting of 1 mL PBS (20  $\mu$ L each) (shown in Figure 3c) onto the PEMs. The modified skin-dermis was, subsequently, incubated in multiwell plates for 1 – 3 days in excess PBS solution on shaker plates. Fluorescent micrographs ( $n = 21$ ) showed that  $98.4 \pm 1.4\%$  of the PEMs remained adhered to skin dermis (Figure 3d). Additionally, the adherence of the PEMs on the skin dermis was tested against an external vertically applied pressure ( $\sim 8$  kPa) and lateral abrasion generated by the motion of Telfa dressing (a commonly used non-adherent dressing) at  $\sim 1$  mm/s (Figure S6). In all treatments,  $>95\%$  of the fluorescent area of the PEMs remained intact on the skin dermis, indicating good adherence of the PEMs to the skin dermis. The strong adherence of the nanofilms on soft tissue is attributed to strong physical interactions, such as through Van der Waals interactions between the PEM and tissue surface.<sup>[26]</sup> We note that some cracks were observed in the PEMs with 40.5 bilayers of (PAH/PAA<sub>2.5</sub>) (see Figure S7). However, such cracks were not observed in PEMs with only 10.5 bilayers of (PAH/PAA<sub>2.5</sub>). The presence of the cracks in the thick PEMs, however, did not prevent their efficient transfer onto the skin dermis by the composite microfilms.

The release profile of silver ions in PBS from modified skin dermis is presented in Figure 3e. The amount of silver released in 24-hours was  $0.04 \pm <0.01$ ,  $0.20 \pm 0.01$ , and  $0.44 \pm 0.04$   $\mu\text{g cm}^{-2}$  from the dermis modified with the three PEMs constructs described above, respectively. Subsequently, the dermis released none,  $0.07 \pm 0.01$ , or  $0.18 \pm 0.03$   $\mu\text{g cm}^{-2}/\text{day}$  of silver, respectively, for the next 2 days. The total amount of silver released, at saturation, over 6 days was  $0.04 \pm <0.01$ ,  $0.41 \pm 0.01$ , and  $0.80 \pm 0.03$   $\mu\text{g cm}^{-2}$ , respectively. These results suggest that, (i) the rate of release of silver ions from the modified dermis depends on the loadings of silver within the PEMs, and (ii) the total amount of silver released from the dermis was lower than the total loading of silver in the PEMs determined before their transfer on to the dermis. We hypothesize, as described previously,<sup>[16]</sup> that extracellular matrix proteins of the skin graft strongly bind silver ions, decreasing the amount of silver ion released into the buffer solutions.

### 2.3. Antibacterial activity of skin dermis modified with composite PEM/PVA microfilms

Skin dermis (GammaGraft) modified with PEM/PVA microfilms was tested for antimicrobial activity against suspensions of either Gram-positive bacteria (*S. aureus*) or Gram-negative bacteria (*Ps. aeruginosa*). Briefly, biopsy punches (6 mm diameter) of dermis placed at the bottom of the wells of a 96-well plate were incubated with 100  $\mu\text{L}$  HBSS containing  $\sim 10^7$  CFU of bacteria on a shaker plate (150 rpm) in a humidified incubator at 37°C. Negative controls in each experiment were no skin dermis, unmodified skin dermis, and skin dermis modified with PEMs without silver. Viable bacterial counts remaining in suspensions were determined by plating, and are reported as colony forming units (CFU).

Bacterial counts in suspension after 24 h and 48 h incubation are summarized in Figure 4. Dermis modified by PEMs with no silver, or PEMs with  $0.04 \pm <0.01$   $\mu\text{g cm}^{-2}$  of silver resulted in bacterial counts in suspensions that were similar to unmodified skin dermis (as shown in the first two columns of Figure 4). The PEMs containing  $1.3 \pm 0.01$   $\mu\text{g cm}^{-2}$  silver caused 3  $\log_{10}$  and 5  $\log_{10}$  CFU decrease in the suspensions within 24 and 48 h, respectively. Finally, the PEMs containing  $2.9 \pm 0.1$   $\mu\text{g cm}^{-2}$  silver caused more than 5  $\log_{10}$  CFU decrease within 24 h of incubation. PEMs with this latter silver loading also mediated a 5  $\log_{10}$  CFU decrease in bacterial counts in suspensions of *Ps. aeruginosa* (Figure S8). We note here that the dermis modified with PEMs containing  $2.9 \pm 0.1$   $\mu\text{g cm}^{-2}$  silver was found to release only  $0.44 \pm 0.04$   $\mu\text{g cm}^{-2}$  of silver in PBS within 24 h (see Figure 3e). This amount of silver ( $\sim 0.4$   $\mu\text{g cm}^{-2}$ ) is sufficient to have a potent antibacterial effect, but, as reported previously,<sup>[17]</sup> allows normal growth and proliferation of NIH 3T3 mouse fibroblast cells.<sup>[17]</sup>

In summary, the *in vitro* experiments described above demonstrate that PEM/PVA microfilms that adhere to the surface of human cadaver skin dermis release sufficient silver in 24 h and 48 h to cause a  $>5$   $\log_{10}$  CFU decrease in bacterial counts in suspensions of *S. aureus* and *Ps. aeruginosa*. These constructs of (PAH/PAA<sub>2,5</sub>)<sub>10,5</sub> were subsequently prepared with a range of silver loadings (including higher loadings achieved by repeated silver ion exchange and reduction cycles, see above) to provide sustained release of antibacterial silver from contaminated murine wound beds described below.



#### 2.4. Modification of excisional wounds in mice using PEM/PVA microfilms

All *in vivo* experiments were performed in an excisional full-thickness wound model in mice, as described in the Experimental section. Briefly, wounds (diameter 6–8 mm) were surgically created on the left and right flanks of mice and were splinted, as described previously<sup>[31]</sup> and shown in Figure 5a. The wounds were ‘splinted’ to minimize wound closure by contraction and, thus, allow wound closure primarily by epithelialization as in human dermal healing.<sup>[31]</sup> Initial *in vivo* studies determined the transfer and persistence of PEMs on the wound-bed. Freshly prepared surgical wounds (6 mm diameter) were allowed to exude excess fluid for 5 min and then were covered with the PEM/PVA microfilms, with the PEMs facing the wound-bed, as shown in Figure 5a. Briefly, the edge of the composite microfilm was held firmly in tweezers and one edge was brought into contact with the wound-bed. Release of the microfilm from the tweezers resulted in adherence of the remaining film to the wound-bed. The PVA cast of each microfilm was observed to start dissolving immediately after contact with the moist wound environment. The PEMs were found to adhere conformally to the wound-bed within 10 min for dissolution of the PVA cast of the composite microfilms, as shown in Figure 5b.

Transfer of the PEMs onto the wound-bed using the PEM/PVA microfilm was quantified using fluorescent microscopy and PEMs assembled using FITC-labeled PAH (as in studies with skin dermis described above). Fluorescent micrographs of FITC-PEMs in Figure 5c–e depict the transfer and persistence of PEMs on murine wounds for up to 3 days post-surgery. To quantify the amount of PEM adhered initially to the wound-bed, wounds were harvested within 30 minutes of treatment and imaged to measure the fluorescent area ( $n = 4$ ). These measurements revealed that the area of the wound covered by the PEM was  $107 \pm 5$  % of the area of the PEM/PVA microfilm prior to transfer onto the wound (shown in Figure 5c,d). This result suggests minor stretching of the PEMs may occur on the elastic tissue surface during harvesting and sample preparation. The PEMs, however, remained firmly attached on the wound-bed.

In one set of mice, splinted wounds modified with fluorescent PEMs were allowed to heal for 3 days and then harvested for fluorescent imaging. After deposition of these PEMs, the wounds were covered with a plastic cover slip such that the cover slip did not touch the wound-bed but prevented external disturbance to the wound-bed (such as scratching by mice). In addition, an aluminum foil was glued over the cover slips to limit exposure to light. The entire construct was then covered with Tegaderm<sup>®</sup>. As shown in Figure 5e, approximately  $90 \pm 2$  % ( $n = 4$ ) of the wound-bed was covered by fluorescent PEMs after 3 days post-immobilization. Approximately 10% of the fluorescent PEM was found to be lost or detached from the tissue surface. We hypothesize that the PEMs are removed from the tissue surface and dispersed as microscopic fragments as the tissue regenerates.

#### 2.5. Reduction in microbial colonization in contaminated wounds modified with silver/PEMs using microfilms

Splinted wounds in mice were topically inoculated with  $\sim 10^6$  CFU *S. aureus* in 10 uL PBS. Following bacterial inoculation, the wounds were treated with the PEM/PVA microfilms (8 mm diameter) and then covered with the biosynthetic wound dressing Biobrane<sup>®</sup> (8-mm

diameter). Sterile nonadherent padding (Telfa) was placed on top of the Biobrane, and the entire construct was secured with Tegaderm (3M). We note here that Biobrane® is a transparent biosynthetic dressing widely used in hospitals for the treatment of burn wounds.<sup>[32,33]</sup> It is composed of a silicone membrane with nylon fibers coated with collagen peptides. Biobrane® seals the wounds and promotes tissue growth.<sup>[32]</sup> A key advantage of Biobrane is that it integrates into wounds and thus circumvents painful dressing changes.<sup>[34,35]</sup> However, it also seals into the wound any peri-wound or endogenous bacteria, resulting in bacterial colonization and failure of therapy in up to 20% of the applications of the dressing.<sup>[36]</sup> Standard of care is to treat wounds with topical solutions of antimicrobial agents before use of Biobrane, or to cover Biobrane with silver dressings that deliver silver to the wound-bed by diffusion across Biobrane. Our objective was to determine if wound-beds modified with silver/PEMs could prevent or reduce bacterial colonization in wounds under Biobrane. Three groups of  $n = 8$  mice each (i.e. a total of 16 wounds/group) were employed: unmodified wounds, wounds modified with PEMs without silver, and wounds modified with PEMs containing silver nanoparticles.

Extrapolating from our *in vitro* studies, we used PEMs of (PAH/PAA<sub>2.5</sub>)<sub>10.5</sub> in mouse experiments. To ensure prolonged release of antimicrobial silver in the murine wounds over 14 days (the average time it takes for complete closure of 6 mm diameter wounds), the silver loading in the (PAH/PAA<sub>2.5</sub>)<sub>10.5</sub> was increased to  $16.8 \pm 0.5 \mu\text{g cm}^{-2}$  by using three cycles of silver ion exchange and reduction, as shown in Figure S9. The silver loading cycles ended with a final silver ion exchange, such that the PEMs provided an initial burst release of silver ions (bound to carboxylic groups of PAA) that was followed by sustained release of silver ions via dissolution of silver nanoparticles entrapped in the PEMs. A typical silver release profile for these PEMs (from PDMS sheets into PBS) is presented in Figure 6. As shown, the PEMs provided an initial burst release of  $3.1 \pm 0.1 \mu\text{g cm}^{-2}$  of silver in the first 24 h, followed by a release of  $\sim 1.5 \mu\text{g cm}^{-2}$  silver/day for 4 days, and a release rate of  $\sim 0.4 \mu\text{g cm}^{-2}$ /day thereafter. The cumulative release of silver over the 30 days period was measured to be  $17.2 \pm 0.6 \mu\text{g cm}^{-2}$ .

Several clinical studies have documented that it takes 48–72 h for Biobrane to integrate into wound-beds.<sup>[34,35]</sup> If wounds are infected during this period, they form exudate pockets under Biobrane where the dressing does not integrate into the wound-bed.<sup>[37]</sup> Therefore, our objective was to demonstrate that modification of contaminated wounds with PEM/PVA microfilms would reduce colonization of *S. aureus* under Biobrane within the first 3 days post-surgery and ensure normal wound closure thereafter. To that end, all mice were euthanized on day 3 post surgery and wounds were harvested, along with the Biobrane, and homogenized for bacterial quantification. Wounds were also imaged on day 0 and day 3 before euthanizing the mice. Figure 7 shows that an average of  $1.8 \times 10^6$  CFU/cm<sup>2</sup> of *S. aureus* was recovered from unmodified wounds on day 3 post surgery. Similarly,  $3.1 \times 10^5$  CFU cm<sup>-2</sup> of *S. aureus* was recovered from the wounds that were modified with PEMs containing no silver. The bacterial burden of wounds in those two groups was not significantly different ( $p > 0.05$ ). In contrast, wounds that were modified by silver/PEMs using the PEM/PVA composite microfilms had an average of only  $6.1 \times 10^3$  CFU cm<sup>-2</sup> of *S. aureus*, i.e. an average of 2.4 log<sub>10</sub> reduction in bacterial burden of the wounds under

Biobrane as compared to unmodified wounds. A repeat experiment with a different batch of silver/PEMs and a larger size of  $n = 10$  mice/group provided evidence of a similar reduction in the microbial burden of the wounds under Biobrane (Figure S10). Overall, these results indicate that modification of wound-beds with silver/PEMs is effective in reducing bacterial colonization of contaminated wounds under Biobrane.

## 2.6. Promotion of normal healing in mice wounds modified with silver/PEMs

The final objective of our study was to demonstrate that modification of wound-beds with silver/PEMs containing  $16.8 \pm 0.5 \mu\text{g cm}^{-2}$  silver (a loading that reduces bacterial colonization of contaminated wounds, see above) does not impair normal healing in clean surgical wounds. Wound healing was monitored until complete wound closure by re-epithelialization (observed within 14 days in all test groups). For these experiments, mice were divided into three groups: a control group with unmodified wounds ( $n = 4$  mice), another control group with wounds modified by PEMs without silver ( $n = 8$  mice), and a test group with wounds modified with silver/PEMs ( $n = 8$  mice). Wounds were covered with a plastic cover slip placed over the splints and the entire construct was covered with Tegaderm®. Mice were monitored daily and wounds were photographed on day 0, 3, 7, 10 and 14 post surgery. Half of the mice in each group were euthanized on day 7 to harvest the wounds for histopathological analysis.

Images of the representative wounds treated with silver/PEMs are shown in Figure 8a–c for post-operative day 0, 7 and 14. Similar representative images for the control groups are shown in Figure S11. These images show, qualitatively, that wounds modified with silver/PEMs exhibited similar rates of wound healing as the controls. The epithelial coverage of the wounds was assessed from digital images of wounds, and is presented in Figure 8d as the percentage of original wound size on post-operative days 3, 7, 10 and 14. A two-way ANOVA analysis was performed (using PRISM software) to determine the effect of two different factors on the size of wounds: (1) time post surgery, and (2) test treatment. It was determined that, (1) time had significant effect on wound size, i.e. wound size at any two time points in each treatment group was significantly different ( $p < 0.0001$ ), and (2) the type of wound treatment had no significant effect on wound size at any time point, i.e. the size of wounds on any particular observation day was not significantly different between the three treatment groups ( $p > 0.05$ ). We also comment that inspection of Figure 8 reveals no evidence of staining associated with the use of silver microfilms.

Representative histopathological sections of the wounds modified with silver/PEMs are presented in Figure 9a–b for day 7 and 14 post-surgery, respectively. Similar representative histopathological images for control wounds are presented in Figure S12. Images at day 7 post-surgery clearly show a migrating re-epithelialization cell layer at the wound edge. In addition, wounds modified with silver/PEMs exhibited re-epithelialization similar to that in control wounds. Complete closure by re-epithelialization was observed in images on day 14. The quality of granulation tissue and degree of inflammation in all tissue sections was found not to be significantly different between the three test groups, suggesting normal progress of wound healing. The epithelial gap in the wounds, measured from histopathological images on day 7 and 14 post-surgery, is presented in Figure 9c as the percentage of initial wound

size. A two-way ANOVA analysis was performed (using PRISM software) to determine the effect of two different factors on the percentage of epithelialization in wounds: (1) time post surgery, and (2) test treatment. It was determined that, (1) time had significant effect on wound epithelialization, i.e. % epithelialization on day 7 and 14 in each treatment group was significantly different ( $p < 0.0001$ ), and (2) the type of wound treatment had no significant effect on % epithelialization at either of the two time points ( $p > 0.05$ ). Overall, these results clearly indicate that modification of the wound-bed using silver-loaded PEM/PVA microfilms (containing  $16.8 \pm 0.5 \mu\text{g cm}^{-2}$  silver) does not cause excessive tissue inflammation and does not impair normal wound healing by re-epithelialization.

### 3. Discussion

This study demonstrates that modification of wound-beds using microfilms comprised of PEMs loaded with silver-nanoparticles and a dissolvable layer of PVA is a promising approach for the management of wound microbial burden. Importantly, following dissolution of the PVA, the conformal contact of the PEMs to the wound-bed enables localized delivery of silver. This reduced the loss of silver in the wound exudate, and thus minimized the need for high silver loadings within the nanofilms.<sup>[17]</sup> This study documents that PEMs releasing up to 100 times less silver than conventional silver dressings (e.g. Acticoat® dressing with nanocrystalline silver release  $\sim 100 \mu\text{g cm}^{-2}$  per day)<sup>[38]</sup> effectively reduced microbial colonization in contaminated murine wounds. Whereas conventional silver dressings (including Acticoat®) have been shown to significantly inhibit re-epithelialization of excisional splinted wounds in mice,<sup>[14]</sup> the loadings of silver used in the PEMs reported in this paper did not inhibit wound re-epithelialization in a similar murine wound-model (as used in<sup>[14]</sup>) and did not cause any excessive inflammation. The PEMs/PVA microfilms could, therefore, potentially be used proactively over clean surgical wounds to prevent microbial infections. In contrast, conventional silver dressings are not recommended for use until a ‘critical colonization’ is established.<sup>[15]</sup> Here we comment that a microbial burden of  $10^5$  CFU/g of tissue or greater in a wound is generally considered equivalent to localized clinical infection.<sup>[1]</sup> In particular, clinical studies with the biologic wound dressing Biobrane® have shown that wounds with greater than  $10^5$  CFU/g of tissue do not permit adherence of Biobrane® to wounds and result in clinical infection.<sup>[54]</sup> Therefore, the result demonstrated in our paper (Fig. 7), namely that use of silver microfilms in contaminated murine wounds reduces the wound microbial burden below  $10^5$  CFU/g of tissue under Biobrane®, is clinically relevant.

The PEM/PVA microfilm constructs used herein for wound microbial management possess a number of additional attributes that make them potentially promising in clinical contexts. (1) The microfilm construct is mechanically strong and translucent, allowing clinicians to easily handle the films and to see through it, thus enabling easy placement on the wound-bed. In contrast, conventional silver-dressings are opaque and must be removed to examine wounds. PEM/PVA microfilms can, thus, potentially reduce patient pain, nursing time, and costs associated with dressing changes. (2) As described earlier, conventional silver dressings are designed to release large concentrations of silver to replenish silver ions lost to proteins in wound fluid.<sup>[39,40]</sup> This results in excessive accumulation of silver aggregates in the epithelium, causing tissue staining and irritation,<sup>[6]</sup> and impairing re-epithelialization.<sup>[14]</sup>

In contrast, the low rates of release of silver from the polymer nanofilms used in this study significantly reduce silver accumulation in the wound, reducing the potential for tissue staining and irritation. (3) As we and others have demonstrated previously, PEMs can be impregnated with an array of bioactive or antimicrobial agents.<sup>[22,41]</sup> The modification of this approach, as described here, represents a significant step in terms of advancing these materials toward a form that is practical for use in a clinical environment with no loss of efficacy of the nanofilm component of the construct. The approach appears, therefore, generalizable to a heterogeneous variety of wounds and to simultaneous release of multiple bioactive agents in wound-beds to support different phases of wound healing. Modification of wound-beds with such PEMs will be explored in future studies.

The results reported in this paper build from previous descriptions of the use of dissolvable films in wounds<sup>[42,43]</sup> by (i) designing and validating a simple procedure for fabrication of silver-loaded microfilm constructs, and (ii) showing that silver-loaded nanofilms immobilized using a dissolvable microfilm construct provide sustained release of low yet therapeutically active levels of silver over weeks. In particular, we contrast our approach to a previous report involving incorporation of an antibiotic.<sup>[44,45]</sup> In that approach, the steps involved (i) formation of a PEM on a substrate and coating of the PEM with a film of PVA; (ii) mechanical removal of the PEM/PVA, inversion of the construct, and replacement attachment of the PEM/PVA constructs onto a substrate with the PEM surface exposed, (iii) deposition of antibiotic (tetracyclin, TC) from acetone onto the surface of the PEM and encapsulation of the deposited layer of acetone by a layer of hydrophobic polyvinylacetate. The authors demonstrated that release of the TC from the construct occurred over 6 hrs in a manner that was dependent on the thickness of the polyvinylacetate layer (layers of polyvinylacetate thicker than 200 nm were reported to delaminate during experiments). In the present study, the fabrication procedure occurs on a single surface, and does not require mechanical removal and replacement of the construct during fabrication. Our approach also does not involve deposition of an hydrophobic barrier layer to control release of the antimicrobial agent. Additionally, we note that a meritorious aspect of our approach is that it also allows controlled release of bioactive agents over 30 days, a period of time that encompasses the time typically involved in wound healing. Finally, we comment that the use of broad spectrum antimicrobial agents such as silver for routine management of microbial burden is advantageous relative to antibiotics such as TC because of the increasing concerns of antibiotic-resistant bacteria. We also note that the silver-loaded PEMs reported in our study appear to be potentially more effective in reducing bacterial colonization both *in vitro* (bacterial reduction of 5.8 and 2.7 log<sub>10</sub> CFU for silver and TC, respectively) and *in vivo* (bacterial reduction of 2.4 and 1 log<sub>10</sub> CFU for silver and TC, respectively) as compared to the PEMs reported by Takeoka et al., although direct comparisons are needed to unambiguously establish the relative performance of the two approaches.<sup>[44,45]</sup>

Finally, we note that our study evaluated, in addition, the efficacy of antimicrobial silver nanofilms in contaminated wounds under Biobrane® dressing. Biobrane was used as an example of a biosynthetic dressing with a high incidence of wound infection rates in patients.<sup>[36]</sup> Because Biobrane exemplifies a primary dressing with high infection rates, the results of our study indicate that wound treatment with silver nanofilms may be broadly

useful for management of microbial burden in combination with a range of moist wound dressings such as silicon films, collagen scaffolds, hydrogel sheets, hydrofibers, and hydrocolloids. Future studies will investigate the efficacy of silver nanofilms when used in combination with these primary wound dressings to reduce microbial burden in contaminated wounds. We will also evaluate if reduction of microbial colonization (by treatment with silver/PEMs) in contaminated wounds ultimately expedites wound closure as compared to unmodified wounds.

## 4. Conclusion

This study demonstrates key aspects of a new approach to the management of microbial burden in wounds based on the modification of wound-beds with polymer nanofilms that are loaded with silver nanoparticles. Although silver is well-known for its antimicrobial activity, when used in wounds, it can lead to staining, tissue toxicity and delayed wound healing. To address these limitations of silver, a composite microfilm construct was designed and fabricated to contain a sacrificial cast of a non-toxic polymer laminated with pre-fabricated polymer nanofilms. This paper documents the successful transfer of >99% of the pre-fabricated, silver-loaded polymer nanofilms onto model wound surfaces using the microfilm constructs. *In vitro*, the silver nanofilms immobilized on human skin dermis reduced >5 log<sub>10</sub> CFU of *S. aureus* and *Ps. aeruginosa*, while releasing <1 μg cm<sup>-2</sup> silver per day. *In vivo*, in splinted wounds in mice, the silver nanofilms provided sustained release of ~1 μg cm<sup>-2</sup> silver per day. This significantly reduced colonization of *S. aureus* under a biosynthetic dressing (Biobrane), as compared to unmodified wounds, 3 days post-surgery. Moreover, in uncontaminated wounds in mice, the modification of wound-beds with the silver nanofilms did not inhibit re-epithelialization nor cause excess inflammation compared to unmodified wounds. Overall, this study validates a facile approach for modification of wound-beds with polymer nanofilms that does not impair wound healing but significantly reduces the loadings of antimicrobial agents needed to manage wound microbial burden as compared to conventional dressings.

## 4. Experimental Section

### Materials

PAH (Mw = 65 kDa), sodium borohydride, and PVA (Mw = 13–23 kDa, 98% hydrolyzed) were obtained from Sigma Aldrich (St. Louis, MO), silver nitrate from Alfa Aesar (Ward Hill, MA), and PAA (Mw = 50 kDa) from Polysciences (Warrington, PA). For the fluorescent study, PAH was labeled with fluorescein-5-isothiocyanate (FITC), Ext/Em-492/518, (Sigma Aldrich) using procedures described elsewhere.<sup>[46]</sup> Polished silicon wafers were purchased from Silicon Sense (Nashua, NH). Terminally gamma irradiated human cadaver skin allograft, GammaGraft®, was obtained from Promethean LifeSciences Inc, Pittsburgh, PA. All work with GammaGraft was performed under sterile conditions in an airflow hood.

### Cleaning of silicon wafer or glass slides

Glass microscope slides and silicon wafers were cleaned sequentially in acidic piranha solution [70:30 (% v/v) H<sub>2</sub>SO<sub>4</sub>: H<sub>2</sub>O<sub>2</sub>] and alkaline piranha solution (70:30 (% v/v) KOH:

H<sub>2</sub>O<sub>2</sub>) for 1 h at 80°C, according to published procedures.<sup>[47]</sup> When required, cleaned glass slides and silicon wafers were coated with octadecyltrichlorosilane (OTS) (using procedures described elsewhere<sup>[48]</sup>) to generate a low-energy surface.

### Preparation of PEMs

Poly(dimethylsiloxane) (PDMS) sheets were fabricated by curing Sylgard 184 (10:1 base to catalyst; Dow Chemical, Midland, MI) on OTS-functionalized silicon wafers or glass slides at 60°C for 24 h. After 24 hours, PDMS was released from the silicon wafers/glass slides and PEMs were assembled on the side of the PDMS that previously was in contact with the OTS-coated silicon wafer/glass slide. The OTS-coated silicon wafer was used to ensure formation of a smooth surface on each PDMS sheet. Aqueous solutions of polyelectrolytes were adjusted to the desired pH using either 1 M HCl or 1 M NaOH for layer-by-layer assembly. The PEMs were assembled on PDMS sheet using a StratoSequence IV, a robotic dipping machine, from nanoStrata Inc, Tallahassee, FL. The PDMS sheets were first immersed into a PAH solution (0.01 M) for 10 min followed by three 1 min rinses with deionized water (Millipore, 18.2 MΩ). Next, the substrates were immersed in PAA solution (0.01 M) for 10 min followed by the rinsing steps described above. The adsorption and rinsing steps were repeated until the desired number of multilayers was deposited, as described elsewhere.<sup>[16]</sup> Post fabrication, the PEMs were dried in vacuum at 60 °C for 1 hour and then stored at ambient conditions.

### Characterization of PEMs

An Olympus IX70 inverted microscope equipped with Chroma Technology Corp. (Rockingham, VT) fluorescence filter cubes was used to image the fluorescence from fluorescent PAH. Images were captured and analyzed using the Metavue version 7.1.2.0 software package (Molecular Devices, Toronto, Canada). A Gaertner LSE ellipsometer ( $\lambda = 632.8$  nm,  $\psi = 70^\circ$ ) was used to measure the thickness of PEMs prepared on silicon wafers. The effective substrate parameters ( $n_s = 3.85$ ,  $k_s = -0.02$ ) were obtained by averaging twelve measurements on the silicon wafers. The refractive index of the PEMs was assumed to be 1.55.<sup>[49]</sup>

### Loading of silver nanoparticles in PEMs and quantification of silver release from PEMs

Synthesis of silver nanoparticles (AgNPs) within the PEMs was initiated by incubation of the pre-assembled PEMs on PDMS in an aqueous solution of AgNO<sub>3</sub> (10 mM) for 1 h, followed by rinsing in water. As described in past reports,<sup>[23,50]</sup> Ag<sup>+</sup> ions diffuse into the PEMs and exchange with the carboxylic protons of the PAA. The carboxylate-bound Ag<sup>+</sup> ions within the PEMs were subsequently reduced to form Ag(0) nanoparticles by incubating PEMs in aqueous NaBH<sub>4</sub> (2 mM) solution for 1 min and again rinsing with water.<sup>[51]</sup> In addition to forming the AgNPs, the acidic solutions conditions regenerate the carboxylic acid groups within the PEMs. This allows additional Ag<sup>+</sup> to be loaded into the PEMs. Repeated incubation in Ag<sup>+</sup> solutions followed by reducing agent solutions can be used to increase the loading of silver in the PEMs.

The loading of silver incorporated into the PEMs was determined by extracting the silver from the PEMs (which were punched into circles of 6 mm diameter using a biopsy punch)

into 2% nitric acid (5 mL) by incubation for 24 h. The concentration of Ag<sup>+</sup> extracted from the PEMs was measured by elemental analysis using an inductively coupled plasma (ICP) emission spectrometer (Perkin Elmer Optima 3000 DV) at the wavelength of 328.068 nm.<sup>[52]</sup> The detection limit of the instrument was specified to be ~0.1 ppb. Details regarding the analytical method can be found elsewhere.<sup>[17]</sup>

Similarly, the release of silver from the PEMs into aqueous solution was quantified by ICP. Sample substrates were individually placed into 15 mL centrifuge tubes, immersed in PBS buffer (3 mL) and incubated without agitation. Substrates were removed daily and placed into new vials containing fresh PBS to simulate sink conditions, with at least 3 samples prepared per experimental group. For ICP analysis, 1 mL of solution from each vial was combined with 2 mL of 3% nitric acid.

### Preparation and release of PEM/PVA microfilms

PVA (25–50  $\mu$ L, 2.5 wt.%) was deposited over PEMs (loaded with or without AgNPs) supported on PDMS sheets (6–8 mm diameter) by spin coating at 1500 rpm (ac=27) for 10s (WS-400A-6NPP/Lite, Laurell Technologies, North Wales, PA). The PEM/PVA microfilm construct was then dried in an oven for 5 min at 70°C. Following drying, the microfilm was peeled from the PDMS surface using tweezers starting from the edge of microfilm. For fluorescent PEMs, the drying step was performed at ambient temperatures for at least 30 min to avoid quenching of fluorescent molecules.

### In vitro antibacterial activity

*S. aureus* (ATCC 6538) and *Ps. aeruginosa* (ATCC 27853) were obtained from ATCC (Manassas, VA). Bacteria were grown in Tryptic Soy Broth Yeast Extract (TSBYE) (BD, Franklin Lakes, NJ) overnight at 37°C with shaking at 200 rpm until a cell density of approximately  $4 \times 10^9$  CFU/mL was reached. The cell density was calculated from a standard curve for optical density (600 nm) of bacterial suspensions prepared using a UV–Vis spectrometer (Beckman Coulter, Fullerton, CA). The bacterial suspensions were centrifuged at 4000 rpm for 10 min and the pellet washed and resuspended in Hank's Balance Salt Solutions (HBSS) buffer. For antibacterial assays, the test samples: 1) GammaGraft without PEMs, 2) PEMs without silver on GammaGraft, and 3) PEMs with silver on GammaGraft, were placed at the bottom of the wells of 96-well plates and were incubated with 100  $\mu$ L PBS buffer (pH 7.4) containing  $10^7$  CFU of bacteria. Plates were incubated with shaking (150 rpm) at 37°C for 24 to 48 h. After the incubation period, the solution in each well was collected in Eppendorf tubes pre-filled with 900  $\mu$ L of ice cold PBS to make a 1 mL suspension of bacteria. To ensure collection of most of the bacteria present in the well, each well was rinsed twice with 200  $\mu$ L diluted bacterial solution collected previously. The viable bacterial cells in the washings were determined by a surface spread-plate method.<sup>[53]</sup> Dilutions of the samples were prepared in PBS and 100  $\mu$ L of each diluted sample was spread onto Trypticase Soy Blood Agar plates (#221261, BD, Franklin Lakes, NJ). After incubation in a 37°C incubator for 24 h, bacterial colonies were counted and used to calculate the mean colony forming units (CFU) per mL. All assays were carried out on at least three different days, with at least three replicates of each test sample performed on each day.



### In vivo antibacterial and wound healing study in mice full-thickness wound model

All experimental protocols were approved by the Institutional Animal Care and Use Committee (IACUC) of the School of Veterinary Medicine, University of Wisconsin-Madison. Phenotypically normal male mice (heterozygous for *Lepr<sup>db</sup>*, Jackson Laboratories, Inc.) or BALB/c mice, 8–12 weeks old, were used in this study. In order to prevent other mice from disturbing the wounds, mice were housed individually in ventilated cages. All mice were acclimatized for a minimum of one week before the surgery. Throughout the study period, mice were maintained in a temperature-controlled facility with a standard light/dark cycle. All mice were provided with environmental enrichment and food and water *ad libitum*. Mice were randomly assigned to either control or experimental groups on the day of surgery. For wounding, mice were anaesthetized with inhaled isoflurane, administered using an induction chamber. After buprenorphine (0.001 mg) delivery to the mice (used for pain control), hair on the left and right thorax immediately behind the shoulder was removed using electric clippers. The area was swabbed with 4% chlorhexidine gluconate surgical scrub alternating with 0.9% sterile saline (3 times each). Subsequently, silicone O-rings (McMaster-Carr, inner diameter 11 mm, outer diameter 15 mm) were applied to the skin 4-mm caudal to the base of the ears on each side of the dorsal midline and secured with tissue glue (Tissumend II) and six 5–0 interrupted nylon sutures. Two 6 mm diameter full thickness excisional wounds were created on the back of each mouse using a biopsy punch. Wounds were centered in the skin circumscribed by the O-ring. O-ring splint application was used to decrease contracture of the wound margins over the course of the study.<sup>[31]</sup> Following wounding, 8 mm diameter PEM/PVA composite microfilms (held in tweezers) were placed onto the wound-beds. Wounds were covered with secondary dressings, as described in the text. Mice were recovered from anesthesia on a warming pad. Wounds were photographed using a digital camera and body weights of mice were registered on post-operative day 1, and every 2–3 days thereafter until the end of the study. Upon completion of the study, mice were euthanized by intra-peritoneal injection of Beuthanasia®-D (Schering-Plough) solution (0.5 mL/mouse) after induction of anesthesia.

For the wound healing study, the splints and sutures were monitored daily for the duration of the study. Similar to our previous animal study,<sup>[54]</sup> any loss of contact between the splint and skin was repaired with glue. Broken or missing sutures were replaced under anesthesia as described above, and a dose of buprenorphine was administered subcutaneously for pain control. Wounds were removed from analysis if two or more sutures were broken or missing within a 24-hour period. Wounds were digitally traced in the photographs and the area calculated using NIH ImageJ software. Wound closure was calculated at each time point as the percentage of the original wound area.

For evaluation of antibacterial efficacy, each wound was inoculated with 10  $\mu$ L of a bacterial suspension containing  $\sim 10^6$  CFU of *S. aureus*. After the bacterial suspension was incubated on the wound for 15 min, the PEM/PVA microfilms (8 mm diameter) were applied to the surgical site and covered with an 8-mm disc of Biobrane® (UDL Labs). PEM/PVA microfilms (with and without silver) and Biobrane were sterilized by UV light for 30 minutes before application to the wounds. Sterile non-adherent padding (Telfa) was placed on top of the Biobrane, and the entire dressing construct was covered with Tegaderm (3M).

These covers were used to protect the wound from rubbing and to create a moist environment to encourage bacterial growth. Mice were recovered from anesthesia on a warming pad. After three days, the mice were euthanized. The wounds (including the Biobrane cover) were harvested with a 6-mm biopsy punch, placed into an Eppendorf tube with 1 mL sterile PBS, and homogenized with a bullet blender for 15 minutes. The viable bacterial cells in the homogenate were determined by a surface-spread plate method as described in the *in vitro* assay.

### Histological examinations

On day 7 post-operative, 2, 5 and 5 mice from the group without microfilms, from the group with microfilms without silver, and from the group with microfilms with silver, respectively, were euthanized. On day 14, after operation, 2, 3 and 3 mice from each group, respectively, were euthanized. For the histopathological study, the entire wound with adjacent normal skin was excised and fixed in 10% buffered formalin. The specimen included the epidermis, dermis and the subcutaneous tissue. Excised wound sites fixed in formalin were processed and embedded in paraffin, and wound sections were stained with hematoxylin and eosin (H&E). Under light microscopy, the H&E sections were photographed using a mounted digital camera (Olympus DP72, Melville, NY) and images were analyzed using an image analysis software (CellSence Dimension 1.4, Olympus, Melville, NY) for length of re-epithelialization, epithelial gap, amount of fibrovascular proliferation in the dermis, and inflammatory response.

### Statistical analysis

Data are presented as means with standard error of the mean (SEM) as error bars, calculated for three or more data points. Significant difference between two groups were evaluated by Student's t-test. Significant difference between more than two groups were evaluated by two-way ANOVA using GraphPad Prism 4 software (GraphPad Software, La Jolla, CA). The level of significance was set at  $p < 0.05$ .

### Supplementary Material

Refer to Web version on PubMed Central for supplementary material.

### Acknowledgments

We thank Tyler B. Nelson for assistance in fabrication/characterization of PEMs and Nancy G. Faith for help with antibacterial experiments. The funding for this study was provided by NIH grant 1RC2AR058971-01 from NIAMS, an Innovation & Economic Development Research grant from the University of Wisconsin-Madison Graduate School, and grants from the Army Research Office (W911NF-10-1-0181 and W911NF-11-1-0251). AA, MJS, CJM, JFM, CJC and NLA possess financial interests in Wound Engineering LLC and/or Imbed Biosciences Inc., for-profit organizations that have filed patent applications and/or are commercializing aspects of the work reported in this publication.

### References

1. Browne AC, Vearncombe M, Sibbald RG. *Ostomy Wound Manage.* 2001; 47:44. [PubMed: 11890078]
2. Ha U, Jin S. *Infect Immun.* 1999; 67:5324. [PubMed: 10496912]
3. Landis SJ. *Adv Skin Wound Care.* 2008; 21:531. [PubMed: 18981758]

4. Dunn K, Edwards-Jones V. *Burns*. 2004; 30:S1. [PubMed: 15327800]
5. Loke WK, Lau SK, Yong LL, Khor E, Sum CK. *J Biomed Mater Res*. 2000; 53:8. [PubMed: 10634947]
6. Atiyeh BS, Costagliola M, Hayek SN, Dibo SA. *Burns*. 2007; 33:139. [PubMed: 17137719]
7. Wu SC, Crews RT, Zelen C, Wrobel JS, Armstrong DG. *Int Wound J*. 2008; 5:416. [PubMed: 18205786]
8. Elzinga G, van Doorn J, Wiersema AM, Klicks RJ, Andriessen A, Alblas JG, Spits H, Post A, van Gent M. *J Wound Care*. 2011; 20:280. [PubMed: 21727877]
9. Jurczak F, Dugré T, Johnstone A, Offori T, Vujovic Z, Hollander D. *Int Wound J*. 2007; 4:66. [PubMed: 17425549]
10. Wright JB, Lam K, Hansen D, Burrell RE. *Am J Infect Control*. 1999; 27:344. [PubMed: 10433674]
11. Poon VKM, Burd A. *Burns*. 2004; 30:140. [PubMed: 15019121]
12. Hidalgo E, Dominguez C. *Toxicol Vitro*. 2001; 15:271.
13. Cho Lee A-R, Leem H, Lee J, Park KC. *Biomaterials*. 2005; 26:4670. [PubMed: 15722137]
14. Burd A, Kwok CH, Hung SC, Chan HS, Gu H, Lam WK, Huang L. *Wound Repair Regen*. 2007; 15:94. [PubMed: 17244325]
15. Hermans MH. *Am J Nurs*. 2006; 106:69.
16. Agarwal A, Guthrie KM, Czuprynski CJ, Schurr MJ, McAnulty JF, Murphy CJ, Abbott NL. *Adv Funct Mater*. 2011; 21:1863.
17. Agarwal A, Weis TL, Schurr MJ, Faith NG, Czuprynski CJ, McAnulty JF, Murphy CJ, Abbott NL. *Biomaterials*. 2010; 31:680. [PubMed: 19864019]
18. Yoo D, Shiratori SS, Rubner MF. *Macromolecules*. 1998; 31:4309.
19. Choi J, Rubner MF. *Macromolecules*. 2005; 38:116.
20. Fu J, Ji J, Yuan W, Shen J. *Biomaterials*. 2005; 26:6684. [PubMed: 15946736]
21. Chua PH, Neoh KG, Kang ET, Wang W. *Biomaterials*. 2008; 29:1412. [PubMed: 18190959]
22. Boudou T, Crouzier T, Ren K, Blin G, Picart C. *Adv Mater*. 2010; 22:441. [PubMed: 20217734]
23. Wang TC, Rubner MF, Cohen RE. *Langmuir*. 2002; 18:3370.
24. Lee D, Cohen RE, Rubner MF. *Langmuir*. 2005; 21:9651. [PubMed: 16207049]
25. Stroock AD, Kane RS, Weck M, Metallo SJ, Whitesides GM. *Langmuir*. 2003; 19:2466.
26. Fujie T, Matsutani N, Kinoshita M, Okamura Y, Saito A, Takeoka S. *Adv Funct Mater*. 2009; 19:2560.
27. Okamura Y, Kabata K, Kinoshita M, Saitoh D, Takeoka S. *Adv Mater*. 2009; 21:4388.
28. Nuttelman CR, Henry SM, Anseth KS. *Biomaterials*. 2002; 23:3617. [PubMed: 12109687]
29. Schmedlen RH, Masters KS, West JL. *Biomaterials*. 2002; 23:4325. [PubMed: 12219822]
30. Jiang Y, Schädlich A, Amado E, Weis C, Odermatt E, Mäder K, Kressler J. *J Biomed Mater Res Part B Appl Biomater*. 2010; 93:275. [PubMed: 20119945]
31. Galiano RD, Michaels J, Dobryansky M, Levine JP, Gurtner GC. *Wound Repair Regen*. 2004; 12:485. [PubMed: 15260814]
32. Whitaker IS, Prowse S, Potokar TS. *Ann Plast Surg*. 2008; 60:333. [PubMed: 18443516]
33. Lang EM, Eiberg CA, Brandis M, Stark GB. *Ann Plast Surg*. 2005; 55:485. [PubMed: 16258299]
34. Klein RL, Rothmann BF, Marshall R. *J Pediatr Surg*. 1984; 19:846. [PubMed: 6520685]
35. Tavis M, Thornto J, Bartlett R, Roth J, Woodroof E. *Burns*. 1980; 7:123.
36. Nichols K, Moaveni Z, Alkadhhi A, Mcewan W. *ANZ J Surg*. 2009; 79:A7.
37. Greenwood JE, Clausen J, Kavanagh S. *Eplasty*. 2009; 9:243.
38. Taylor PL, Ussher AL, Burrell RE. *Biomaterials*. 2005; 26:7221. [PubMed: 16005512]
39. Trop M, Novak M, Rodl S, Hellbom B, Kroell W, Goessler W. *J Trauma*. 2006; 60:648. [PubMed: 16531870]
40. Mooney EK, Lippitt C, Friedman J. *Plast Reconstr Surg*. 2006; 117:666. [PubMed: 16462356]
41. Lichter JA, Van Vliet KJ, Rubner MF. *Macromolecules*. 2009; 42:8573.

42. Vendamme R, Onoue SY, Nakao A, Kunitake T. *Nat Mater.* 2006; 5:494. [PubMed: 16715083]
43. Cheng W, Campolongo MJ, Tan SJ, Luo D. *Nano Today.* 2009; 4:482.
44. Fujie T, Saito A, Kinoshita M, Miyazaki H, Ohtsubo S, Saitoh D, Takeoka S. *Biomaterials.* 2010; 31:6269. [PubMed: 20493525]
45. Saito A, Miyazaki H, Fujie T, Ohtsubo S, Kinoshita M, Saitoh D, Takeoka S. *Acta Biomater.* 2012; 8:2932. [PubMed: 22525350]
46. Gupta JK, Tjipto E, Zelikin AN, Caruso F, Abbott NL. *Langmuir.* 2008; 24:5534. [PubMed: 18419143]
47. Skaife JJ, Abbott NL. *Chem Mater.* 1999; 11:612.
48. Brake JM, Abbott NL. *Langmuir.* 2002; 18:6101.
49. Lockwood NA, Cadwell KD, Caruso F, Abbott NL. *Adv Mater.* 2006; 18:850.
50. Joly S, Kane R, Radzilowski L, Wang T, Wu A, Cohen RE, Thomas EL, Rubner MF. *Langmuir.* 2000; 16:1354.
51. Logar M, Jancar B, Suvorov D, Kostanjšek R. *Nanotechnology.* 2007; 18:325601.
52. Shi Z, Neoh KG, Zhong SP, Yung LYL, Kang ET, Wang W. *J Biomed Mater Res Part A.* 2006; 76:826.
53. Herigstad B, Hamilton M, Heersink J. *J Microbiol Methods.* 2001; 44:121. [PubMed: 11165341]
54. Guthrie KM, Agarwal A, Tackes DS, Johnson KW, Abbott NL, Murphy CJ, Czuprynski CJ, Kierski PR, Schurr MJ, McAnulty JF. *Ann Surg.* 2012; 256:371. [PubMed: 22609841]
55. Bieker P, Schönhoff M. *Macromolecules.* 2010; 43:5052.

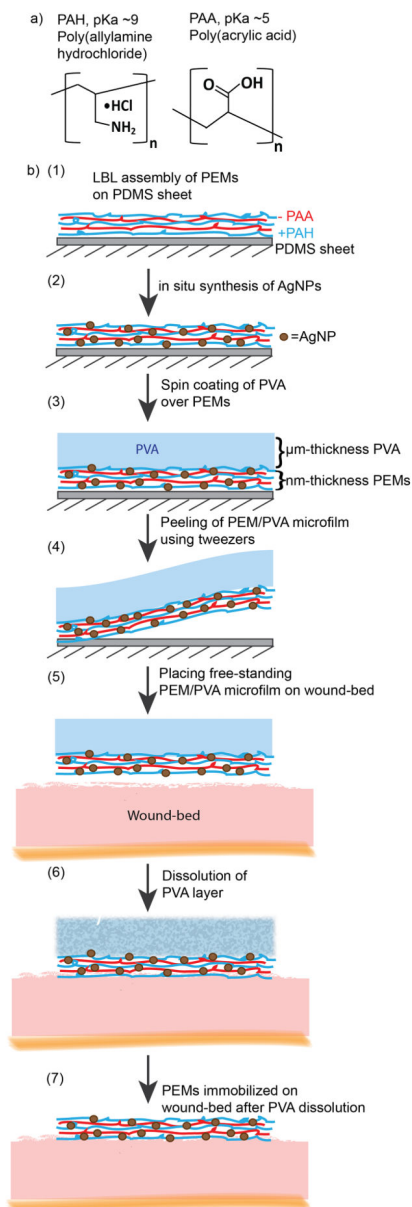


**Figure 1.**

a) Polyelectrolytes employed for layer-by-layer assembly of nanometer-thick PEMs. b) Schematic illustration of the procedure used to fabricate PEM/PVA microfilms and apply them to wound-beds: (1) PEMs are assembled on PDMS sheets, (2) post-fabrication, PEMs are impregnated with silver ions that are subsequently reduced to silver-nanoparticles, (3) PVA solution is spin-coated over silver-loaded PEMs, (4) PEM/PVA microfilm is peeled from the PDMS sheet and (5) placed onto a moist wound-bed. 6) Dissolution of the PVA layer in the moist wound leads to (7) immobilization of the PEMs on the wound-bed.

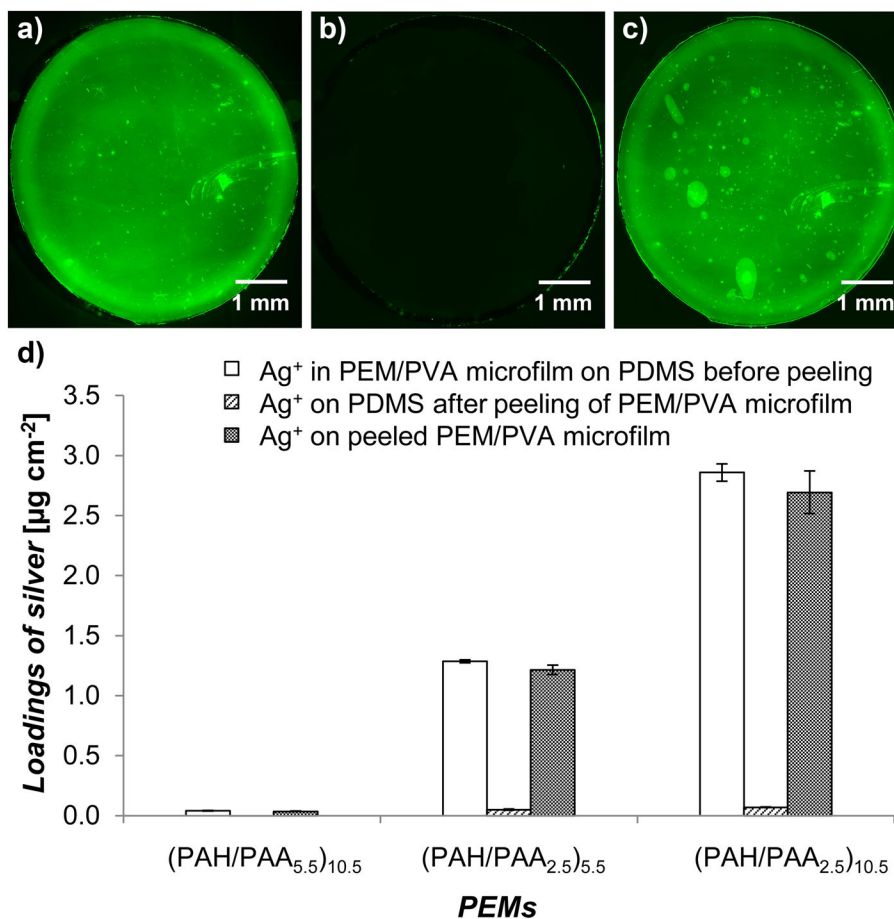


**Figure 2.** Microfilms of PEMs/PVA can be uniformly peeled from PDMS sheets on which they are fabricated and they retain their silver loadings. a–c) Representative fluorescent micrographs of a 6 mm diameter PEM/PVA microfilm with PEMs of (FITC-PAH/PAA<sub>5.5</sub>)<sub>10.5</sub>, (a) PEM on a PDMS sheet before peeling, (b) PDMS after peeling, and (c) PEM placed on a glass slide for imaging. d) Silver loading of PEMs/PVA microfilms before and after peeling the PEMs from the PDMS sheets, illustrated using PEMs with different silver loadings. Data presented as mean  $\pm$  SEM with n = 4.

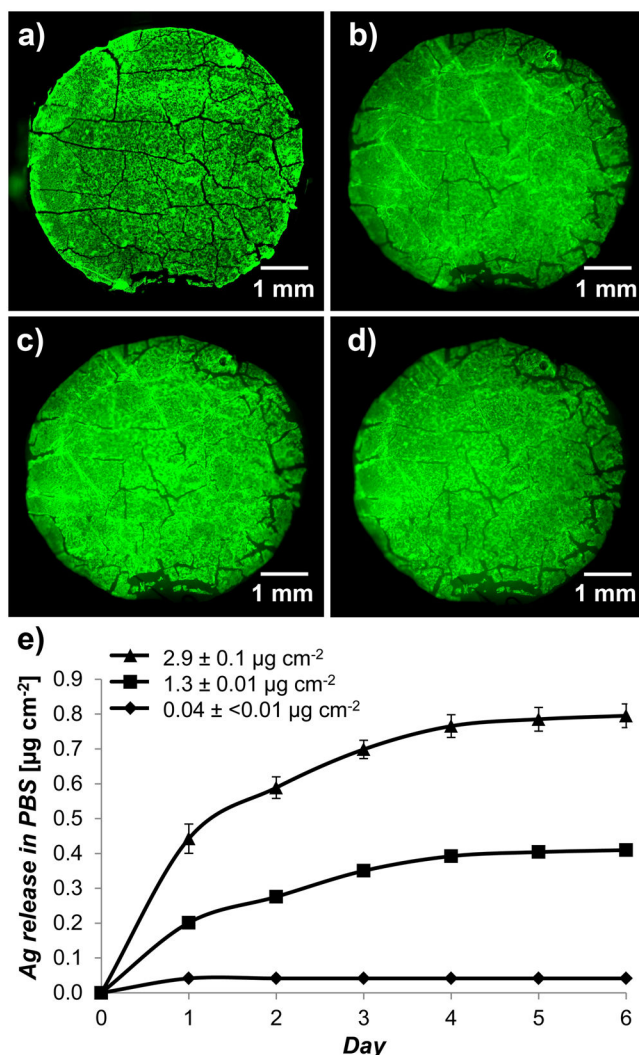


**Figure 3.** Characterization of PEMs immobilized from PEM/PVA microfilms onto human cadaver skin dermis (GammaGraft), which was used to simulate the exposed dermis of a partial thickness wounds. Fluorescent micrographs of (a) microfilm with PEMs (FITC-PAH/PAA<sub>2.5</sub>)<sub>40.5</sub> on PDMS sheet, (b) PEM/PVA microfilm placed onto skin dermis with the PEMs facing the surface of the tissue, (c) PEMs immobilized on skin dermis after repeated rinsing with 1 mL PBS, and (d) PEMs retained on human skin dermis after 3 days of continuous incubation in excess PBS on shaker plates. e) Sustained release of silver ions into PBS from skin dermis modified with PEMs containing a range of silver loadings. The graph shows that the rate of silver ion release increased with the silver loading of the PEMs. Data presented as mean  $\pm$  SEM with n = 4.

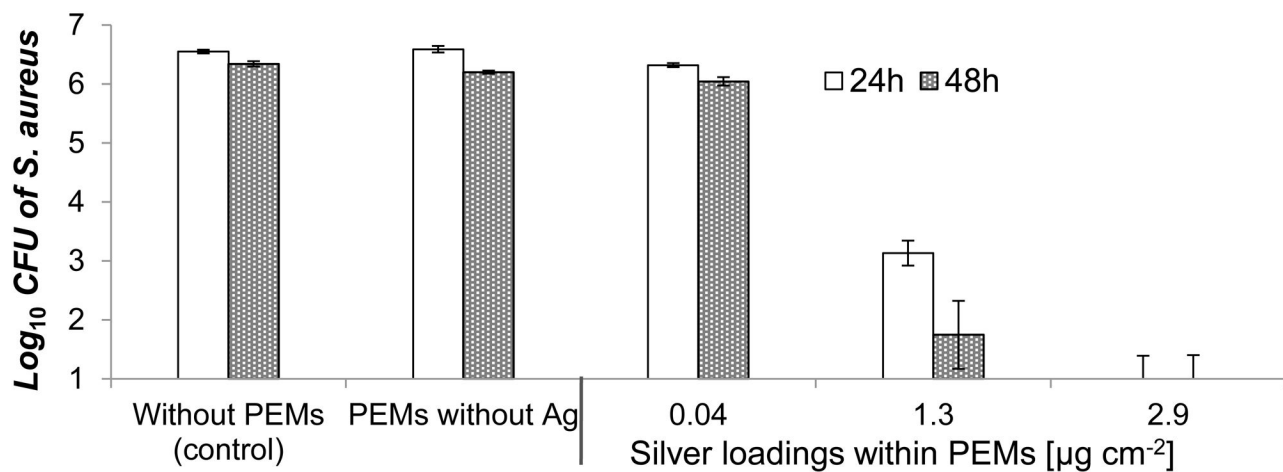


**Figure 4.**

Antibacterial activity in suspensions of *S. aureus* incubated for 24 h or 48 h over skin-dermis modified with PEM/PVA microfilms with a range of silver loadings. Modified skin-dermis was incubated in 96-well plates with  $10^7$  CFU of *S. aureus* in 100 mL HBSS buffer on shaker plates (150 rpm) at 37°C. Data presented as mean  $\pm$  SEM with n = 4.



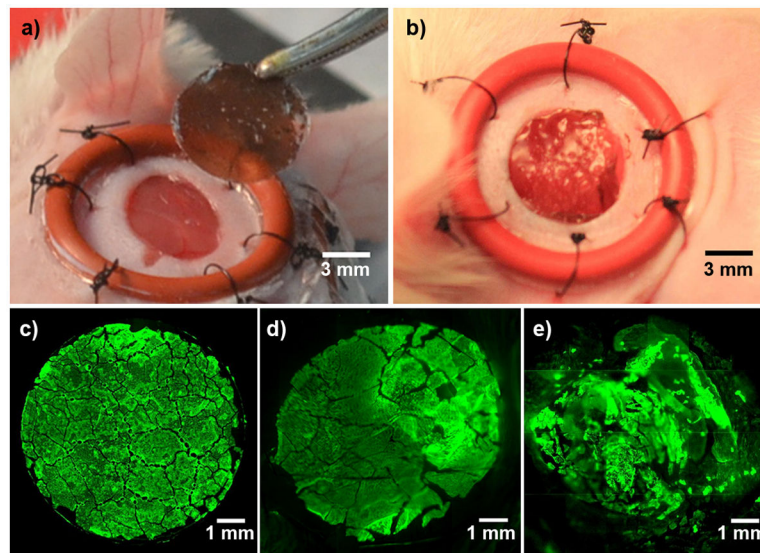


**Figure 5.**

a–b) Modification of full-thickness splinted wound in mice with a silver/PEM using a microfilm. Photograph of (a) splinted wounds in mice with PEM/PVA microfilm held by tweezers, and (b) PEMs adhered on mice wounds. c–e) Characterization of persistence of fluorescence-tagged PEMs immobilized on the surface of excisional full-thickness. Fluorescent micrographs of PEM/PVA microfilm with a PEM of (FITC-PAH/PAA<sub>2.5</sub>)<sub>40.5</sub>, (c) on PDMS sheet before transfer, (d) on wound-bed harvested from mice after 1 h, (e) on wound-bed harvested from mice after 3 days post-surgery.

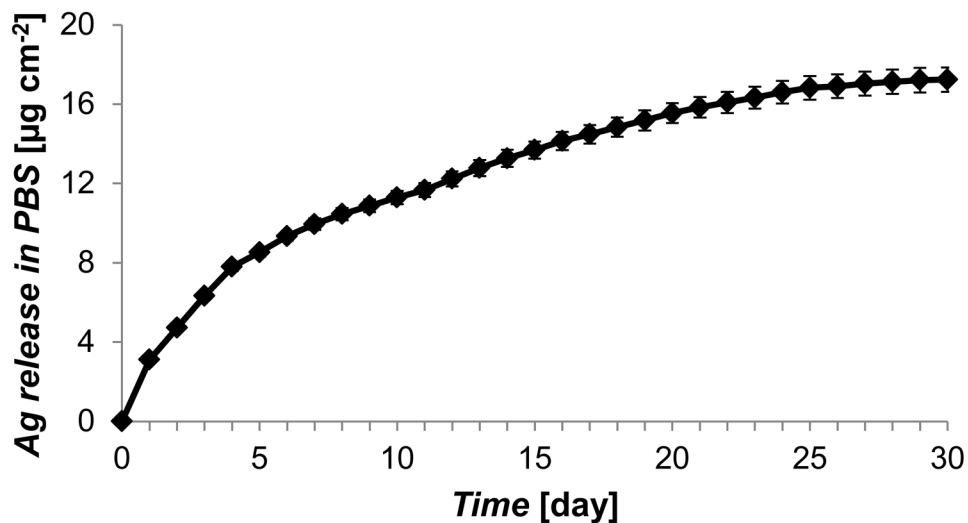


**Figure 6.** Sustained release of silver ions into PBS from PEMs of  $(\text{PAH}/\text{PAA}_{2.5})_{10.5}$  with silver loadings of  $16.8 \pm 0.5 \mu\text{g cm}^{-2}$ . Silver loading in the PEMs was achieved by repeating three cycles of silver ion exchange and reduction. This construct of PEMs was used to treat contaminated wounds in mice. Data presented as mean  $\pm$  SEM with  $n = 3$ .

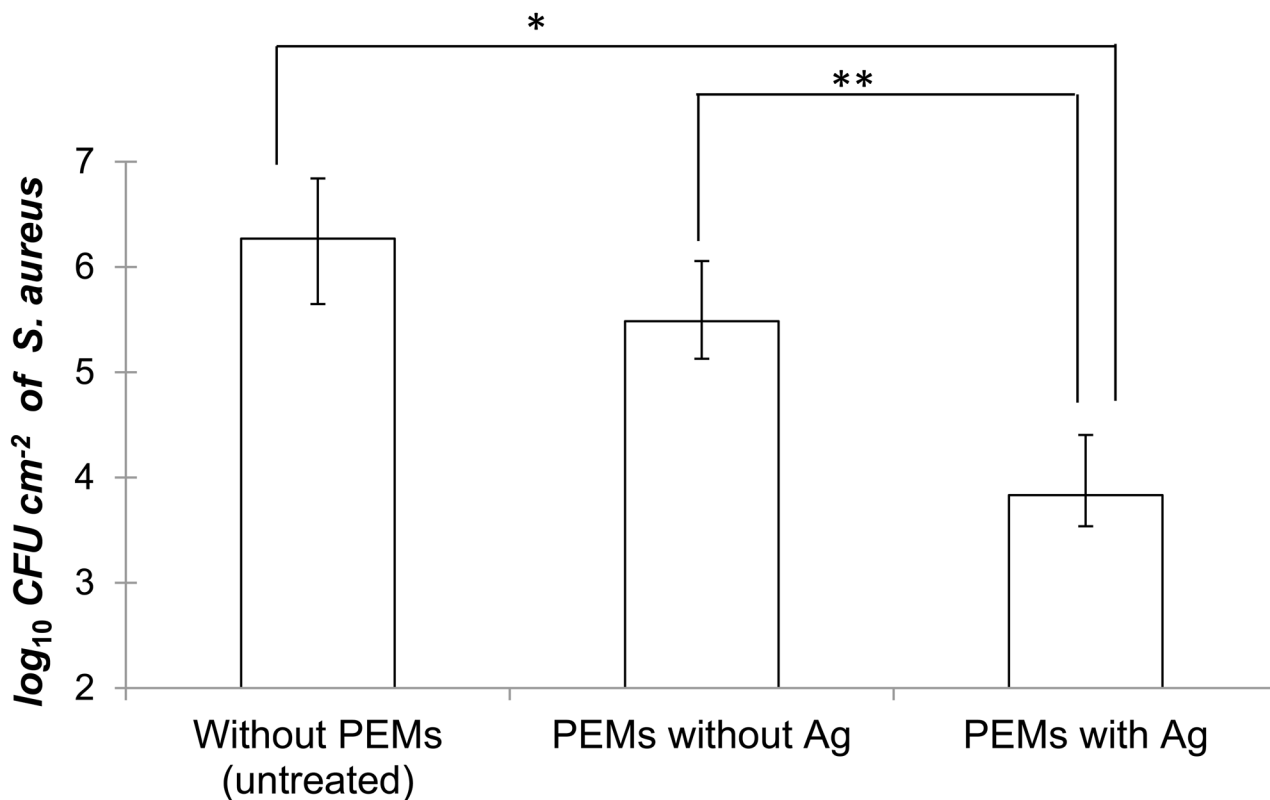


**Figure 7.** Inhibition of microbial colonization in contaminated murine wounds treated with PEM/PVA microfilms (with silver loading of  $16.8 \pm 0.5 \mu\text{g cm}^{-2}$ ). Excisional 6 mm diameter splinted wounds topically inoculated with  $3.0 \times 10^6$  CFU/ $\text{cm}^2$  of *S. aureus* were treated with the PEM/PVA microfilm and covered with a biosynthetic wound dressing Biobrane®. Figure shows bacterial counts recovered from wounds harvested and homogenized (along with Biobrane®) after 3 days post-surgery (\*  $P < 0.001$ , \*\*  $P < 0.05$ ). Data represent the mean  $\pm$  SEM with  $n = 8$  mice (=16 wounds) for each group.

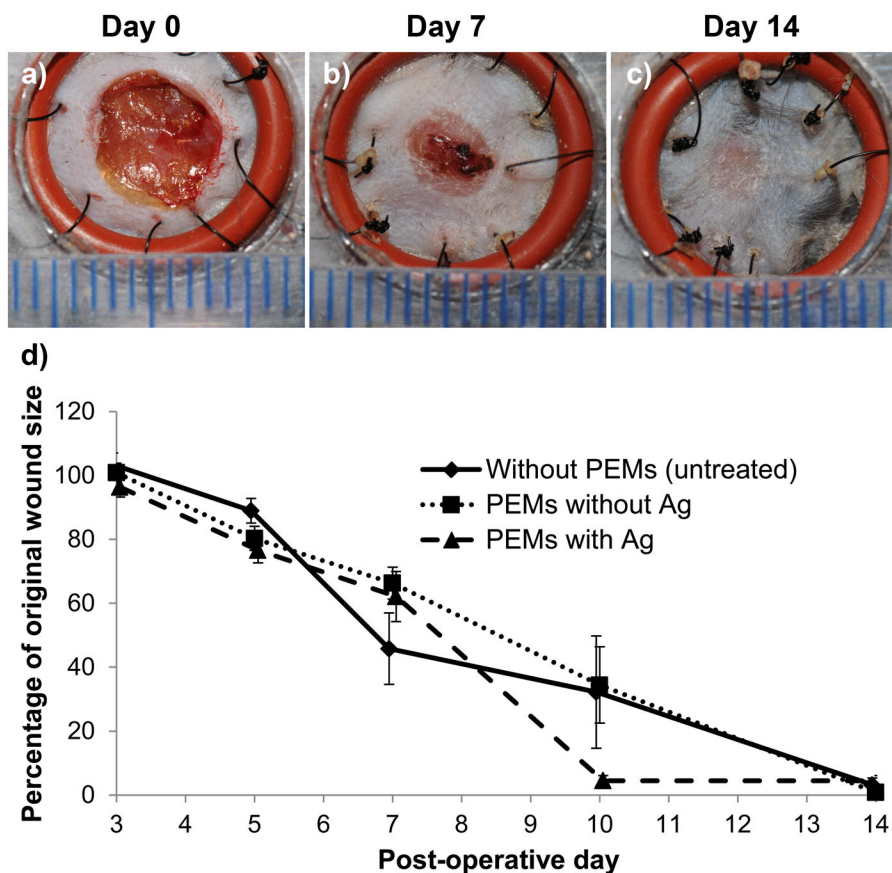


**Figure 8.** PEM/PVA microfilms promote normal wound healing in excisional splinted wounds in mice. Figures (a, b, c) show gross images of wounds on post-operative days 0, 7 and 14, respectively, that were modified post-surgery with silver/PEMs (with silver loading of  $16.8 \pm 0.5 \mu\text{g cm}^{-2}$ ). Each line on the scale represents 1 mm. (d) Percentage of original wound size on post-operative days 3, 5, 7, 10 and 14 in wounds that did not receive PEMs and wounds that were modified with either PEMs containing no silver or PEMs containing  $16.8 \pm 0.5 \mu\text{g cm}^{-2}$  silver. There were no significant difference on wound sizes between the three experimental groups. Each data point presents mean  $\pm$  SEM of relative wound size. The sample size (n) for days 3, 5, and 7 were n = 8, 16 and 16, respectively, for each group. On day 7, some wounds were harvested for histopathology. The sample sizes for the three groups on days 10 and 14 were n = 4, 6 and 6, respectively

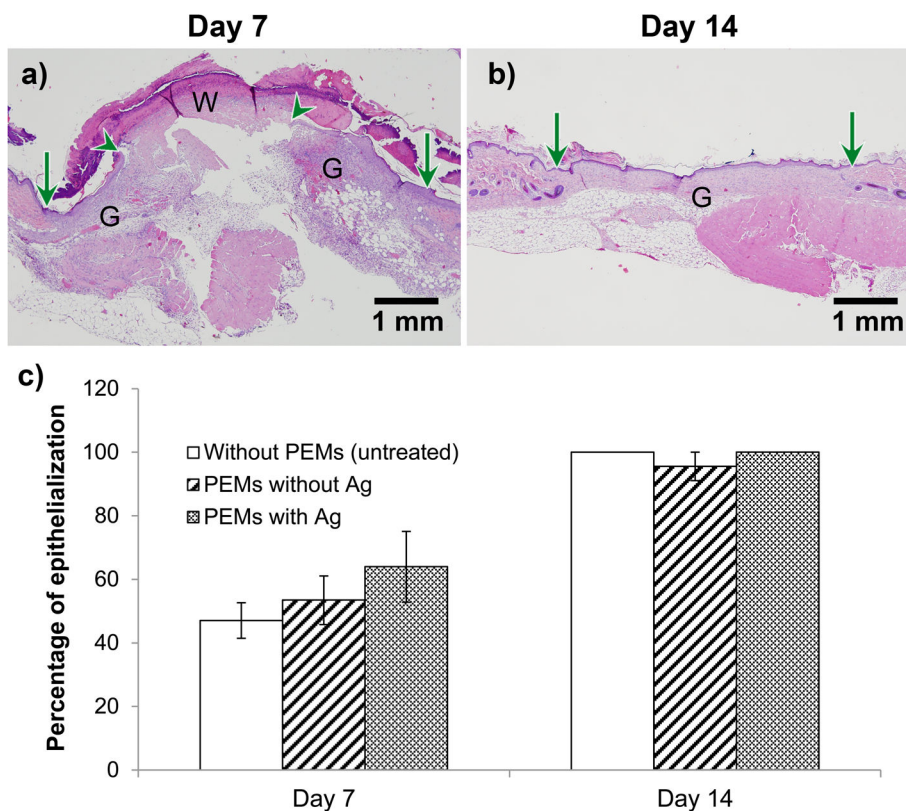


**Figure 9.** PEM/PVA microfilm (with  $16.8 \pm 0.5 \mu\text{g cm}^{-2}$  of silver) promotes epithelialization similar to the untreated wound in excisional splinted wounds in mice, as determined by histopathology. Figures (a, b) show representative H&E-stained sections of wounds postoperative days 7 and 14, respectively, in wounds modified with silver/PEMs. Original wound edge (arrow), migrating epithelial tongue (arrow head), granulation tissue (G), and wound matrix (W) are marked. (c) Percentage of original wound size on post-operative days 7 and 14 in wounds that did not receive PEMs, and wounds that were modified with PEMs containing no silver or PEMs containing silver. Each data point presents mean  $\pm$  SEM of relative wound size. The sample size (n) for day 7 for the groups without PEMs, with PEM/PVA without Ag, and with PEM/PVA with Ag, were n = 4, 9, and 7, respectively. For day 14, n = 3 for each group.